Research Article

João Vitorino, Bruno Damas, Vítor Víegas*

Harvesting energy from a soldier's gait using the piezoelectric effect

https://doi.org/10.1515/EHS-2023-0149
received October 30, 2023; accepted May 12, 2024

Abstract: There is an increasing dependence on electronic devices in the battlefield, including equipment for communications, positioning and navigation, and combat situation awareness. These devices are usually powered by batteries because they are reliable and have good power density (energy per kilogram). Nevertheless, batteries are heavy and bulky, which reduces agility and increases fatigue of the ground troops. An alternative is to extract energy from renewable sources (like the sun and the wind) or harvest energy from the human body itself (like temperature gradients and walking). This article studies the feasibility of a piezoelectric generator, stimulated by human gait, to power electronic devices on the battlefield. Tests were carried out to measure the energy harvested from several piezoelectric ceramics placed under the sole of a soldier's boot. Different materials and arrangements were tried to maximize the power, leading to the development of a prototype. The prototype was able to harvest 875 μJ on each step, on average. Walking 1 h, at a pace of 40 steps/min, leads to 2.1 J of energy, enough to supply a 3.3 V device consuming 10 mA for around a minute. These results are interesting for any situation that requires emergency power on the battlefield (e.g., trigger a device, call for rescue, acquire localization).

Keywords: piezoelectricity, piezoelectric generator, energy harvesting, human gait

*** Corresponding author: Vítor Víegas,** CINAV – Centro de Investigação Naval, 2810-001 Almada, Portugal; IT – Instituto de Telecomunicações, 1049-001 Lisboa, Portugal, e-mail: vitor.viegas@escolanaval.pt
João Vitorino: CINAV – Centro de Investigação Naval, 2810-001 Almada, Portugal, e-mail: amaro.vitorino@marinha.pt
Bruno Damas: CINAV – Centro de Investigação Naval, 2810-001 Almada, Portugal; ISR – Institute for Systems and Robotics, LARSyS, 1049-001 Lisboa, Portugal, e-mail: bruno.damas@escolanaval.pt

1 Introduction

Over the years, military forces have been using electronic aids to conduct operations, leading to a significant increase in the consumption of electrical energy per combatant (Harper 2015). The first electronic aids were introduced to support communications between forces on the ground, and between these and the command center. Since then, electronic aids have been added for geographic location and navigation, night vision, and situational awareness, including the detection and identification, in real time, of the various actors on the ground. More and more electronic equipment is arriving on the battlefield, transforming raw data into useful information that aids the combatant to take the right decisions.

Batteries are the most obvious and efficient solution for powering portable electronic equipment, also on the battlefield. Batteries must be able to store a large amount of energy to maximize autonomy, but batteries with greater capacity are usually bulkier and heavier, which impairs the mobility and agility of the user (Swanner et al. 2017). Thus, it is of great importance to make the batteries smaller and lighter, eventually complementing them with other energy sources, so that the energy needs are met without fatiguing the combatant. The main energy sources available in campaign are the following (Raadschelders & Schmal 1999):

- Electrochemical batteries: These devices are most common in the field because they have good energy densities. Many chemistries are available, from non-rechargeable alkaline batteries based on zinc-manganese dioxide cells to rechargeable batteries based on lead or, more recently, on lithium ions.
- Betavoltaic cells: These devices are a type of nuclear battery that generates electricity when beta particles (electrons), emitted from a radioactive source, radiate a semiconductor (PN) junction. Their main advantage is the ability to work for many years (sometimes decades) providing good amounts of energy. The main drawbacks are the high cost and the risk of environmental and personal contamination.
- Renewables sources: The energy from the sun and the wind is easily converted to electricity using portable

solar panels and wind turbines. The energy is inexhaustible and accessible, but the generators are a bit heavy and bulky.
- Latent energy sources from the surroundings: It is also possible to harvest energy from less obvious sources, including electromagnetic fields (associated with radio signals), temperature gradients (using the pyroelectric effect), and vibrations (common in heavy machinery and piping).

This work studies the possibility of transforming mechanical energy from walking into electrical energy through the inclusion of small piezoelectric generators in military boots. These piezoelectric elements, hidden in the shoe, may be able to produce electricity passively while the dismounted soldier moves around. The energy produced would help to increase the autonomy of existing batteries, eventually enabling their replacement by smaller and lighter batteries, or could be used as emergency backup power.

The direct piezoelectric effect is based on the appearance of an electric voltage in a material subjected to mechanical deformation. This is due to the alteration on the internal electrical charge distribution of an asymmetrical crystalline structure. The redistribution of electrical charge gives rise to the appearance of an excess of charges, positive and negative, on opposite sides of the material. This effect exists in natural crystals, such as quartz, and in certain manufactured ceramics and polymers. Ceramic materials like lead–zirconate–titanate (PZT) have a piezoelectric effect about two orders of magnitude larger than natural crystals and can be produced very economically. On the other hand, the inverse piezoelectric effect consists in the appearance of a deformation caused by an electric voltage applied to the piezoelectric material. Both effects, direct and inverse, are used to build sensing and actuating devices (Heywang et al. 2008).

The electrical behavior of piezoelectric materials can be expressed through the equivalent electrical circuit shown in Figure 1. The circuit is composed by the capacitance C_e that represents the elasticity of the material, the inductance L_m that represents the inertia associated with the mass of the material, the capacitance C_s that represents the static capacity of the material (capacity between electrodes), and the resistance R_s that represents the insulation resistance of the material (Pointon 1982). The frequency response of the circuit is represented on the right in Figure 1, with two distinct zones to be highlighted: a flat zone, preferably used by piezoelectric sensors, where the dominant effects are those of elastic capacity and insulation resistance, and a resonance peak used preferentially by piezoelectric generators.

The size and composition of current piezoelectric materials move the resonance peak to high frequencies (hundreds or thousands of hertz), which is much higher than the frequencies related to human activities. For this reason, it is hard to take advantage of any resonance phenomenon when harvesting mechanical energy from the human body.

1.1 Related work

Many works on piezoelectric generators have been developed, with a substantial increase since the beginning of the century (Sezer & Koç 2021). Most of the authors have been focused on collecting mechanical energy from heavy machinery (Kim et al. 2005), and only a few have studied the problem of harvesting energy from the human body.

Shenck & Paradiso (2001), at the MIT Media Lab, demonstrated energy scavenging from piezoelectric elements placed between the shoe's sole and insole. They used PZT beneath the heel and piezoelectric polymer polyvinylidene-fluoride (PVDF) beneath the ball of the foot. The energy dissipated in the heel was harnessed by flattening a curved, prestressed spring composed by two curve metal strips laminated with PZT. The energy dissipated in bending the ball of the foot was harnessed by compressing and

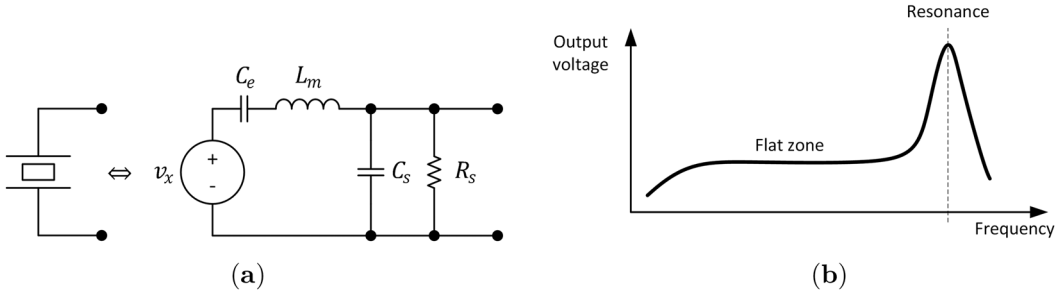

Figure 1: Piezoelectric crystal model: (a) electrical equivalent circuit and (b) corresponding frequency response.

decompressing a PVDF film. In average, per step, the PZT spring produced 9.3 mJ and the PVDF film produced 1.4 mJ.

Granstrom et al. (2007) developed an energy-harvesting backpack capable of generating electrical energy from the forces between the wearer and the pack. They replaced the traditional straps of the backpack with others made of PVDF, which is highly flexible and very strong. The backpack equipped with two piezoelectric straps, loaded with 44 kg, produced, on average, 45.6 mJ per step.

Howells (2009) proposed a mechanism that converts the heel strike into the rotation of a camshaft, which, in turn, hammers four PZT elements alternately. The piezoelectric elements were arranged in such a way that they deflect 90 degrees out of phase with one another, recycling most of the mechanical energy in the heel. On average, the system produced 90.3 mJ per compression.

Rocha et al. (2009) developed an energy harvester composed by a film of PVDF placed under the foot, in the heel region and between the metatarsals and phalanges. The energy generated by deforming the film was dissipated on a matching resistive load. On average, the system produced 3.5 μJ per step.

Ishida et al. (2013) developed a pedometer supplied by 21 PVDF rolls embedded in the insole. The electricity generated by compressing and decompressing the rolls was conditioned by custom-built organic electronics. On average, the system was able to produce 2.6 μJ per compression.

Zhao & You (2014) developed a PVDF-based piezoelectric generator fully integrated into the shoe. The film was placed between two platforms with curved notches that acted as teeth "chewing" the piezoelectric material. On average, the generator was able to deliver 1 mJ of energy per step.

Jung et al. (2015) demonstrated a flexible piezoelectric generator that maximizes the stress/strain distribution. They used a curved leaf spring, with two faces, coated with PVDF film. On each cycle of compression and decompression, the structure generated, on average, 109 mJ, capable of lighting up 476 led bulbs.

Hwang et al. (2015) developed a piezoelectric structure that was able to produce electricity when stepped on. The structure was composed of two platforms between which there were springs and steel blades covered with piezoelectric material. When the structure was compressed, the springs deflected, and the steel blades started to vibrate, thus exciting the piezoelectric material based on PZT. Tests were carried out to tune the mechanical part of the system to its natural frequency and to adapt the electrical load to the condition of maximum energy transfer. Each step generated, on average, 120 μJ of energy.

Kuang et al. (2016) developed a piezoelectric knee-joint energy harvester that used magnets to deform PZT-coated cantilever beams. The rotational nature of the mechanism (driven by the joint), the number of beams (8), and the number of magnets (32) allowed frequency-up conversion, closer to the resonance frequency of the beams. The system was able to generate 6.4 mJ of energy, per step, on average.

Finally, Fan et al. (2017) presented a shoe-mounted harvester consisting of a PZT-coated cantilever beam magnetically coupled to a ferromagnetic ball and a crossbeam. The ball was designed to harness energy from the swing motion, while the crossbeam was designed to harness energy from the heel strike. Together, they were able to produce 287 μJ of energy, per step, on average.

Table 1 summarizes the results of the related work. We see that the values have a high variability, ranging from some micro-Joules to hundreds of milli-Joules. The highest values occur when a dedicated mechanical structure was built to maximize the deformation of the piezoelectric elements. This is a key point that we took into consideration when developing our work, as will be seen later.

1.2 Contributions

In this article, we present a low-cost piezoelectric generator intended to be embedded in military boots. Our

Table 1: Comparison of results

Work	Year	Material	Mean energy per step (μJ)	Reference
Shenck et al.	2001	PZT	9,300 + 1,400	Shenck & Paradiso (2001)
Granstrom et al.	2007	PVDF	45,600	Granstrom et al. (2007)
Howells et al.	2009	PZT	90,300	Howells (2009)
Rocha et al.	2009	PVDF	3.5	Rocha et al. (2009)
Ishida et al.	2013	PVDF	2.6	Ishida et al. (2013)
Zhao et al.	2014	PVDF	1,000	Zhao and You (2014)
Jung et al.	2015	PVDF	109,000	Jung et al. (2015)
Hwang et al.	2015	PZT	120	Hwang et al. (2015)
Kuang et al.	2016	PZT	6,400	Kuang et al. (2016)
Fan et al.	2017	PZT	287	Fan et al. (2017)

proposal, shown in Figure 2, is quite simple as it consists of piezoelectric ceramics encrusted in the boot's insole and a conditioning circuit that collects, stores, and regulates the generated power.

The main contributions of this work are as follows:

(1) A comprehensive study about the best way to connect the piezoelectric elements given the fact that they spread under the foot and are not excited all at the same time during the gait.
(2) The development of easy-to-make mechanical structures that greatly improve the strain of the piezoelectric elements, and
(3) The presentation of an use case of a commercial nano power harvester.

This article is organized as follows: Section 2 describes the development of a piezoelectric generator including all the aspects to optimize its output power. Section 3 evaluates the performance of the developed prototype, and Section 4 extracts conclusions pertaining its practical applicability.

2 Materials and methods

This section describes the development of a piezoelectric generator covering the following topics: (1) choice of the piezoelectric elements, (2) strain optimization, (3) finding of the matched load, (4) placement under the foot, and (5) design of an electronic circuit to store the electricity produced. Each topic will be handled on a dedicated subsection.

2.1 Piezoelectric elements

We chose to use piezoelectric elements from muRata, model 7BB-20-6L0, because they are very common and cheap (Mouser Electronics currently sells them at 0.50 € for a quantity 100+). These piezoelectric elements are in the form of a disc with a diameter of 20 mm with two wires soldered on both sides. The discs are very thin (0.20 mm) and light (844 mg), so they can be easily embedded in the sole of a shoe.

2.2 Strain optimization

A first test was carried out by placing a piezoelectric element in the heel area. The element was placed between two slightly padded insoles, sewn to the lower insole, and protected by the upper insole, all inside a military boot. The output voltage was visualized directly with a digital oscilloscope (Tektronix 1002B) through a 10× attenuation probe. Waveforms were acquired while a midshipman weighing 90 kg made "normal" steps in slow gait.

The first results were somewhat disappointing, with relatively low voltages, not exceeding 9 V peak. It was then hypothesized that the piezoelectric element was not sufficiently deformed and that the mechanical coupling of the element would have to be improved to generate more strain. Six structures were then 3D-printed in polylactic acid (PLA) and attached to the piezoelectric element using general-purpose glue. All structures were carefully designed to optimize strain without compromising the user's comfort.

New tests were carried out to evaluate the performance gains introduced by the PLA structures. Each structure was stimulated with ten steps under the same conditions as earlier (same user, same placement, same boot, similar piezoelectric disks, etc.). The waveforms generated by the piezoelectric elements were acquired by the digital oscilloscope and compared in terms of amplitude. The best results were achieved by the structure shown in Figure 3, with voltages reaching 60 V peak, almost ten times higher than earlier. Figure 4 shows the voltages generated without the PLA structure (dashed line) and with the PLA structure (full line); the performance improvement is evident.

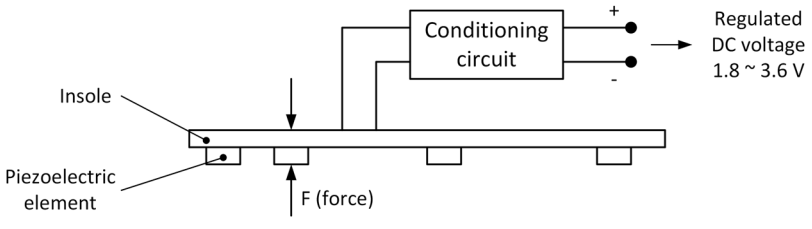

Figure 2: Proposed solution.

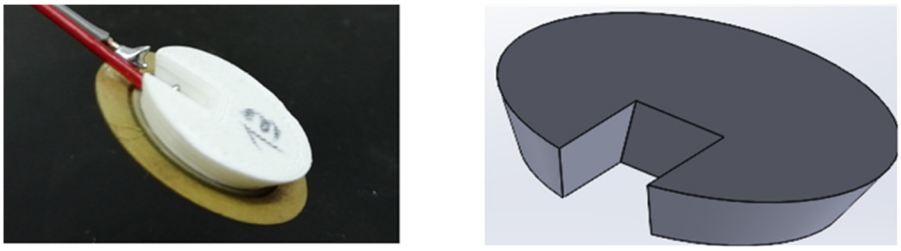

Figure 3: PLA structure printed to optimize the strain of the piezoelectric elements.

2.3 Matched load

Another topic of interest was to find the matched load that maximizes the power transferred from the piezoelectric generator. For that purpose, we inserted the piezoelectric element, enriched with the PLA structure, inside the boot, in the heel region, and connected the terminals to a load resistor (R_L). The typical user made ten "normal" steps, each one with a duration close to 1 s. The voltage across the load resistor (u) was registered by the digital scope, connected through a 10× attenuation probe. The mean power of each step was computed as

$$p_{\text{avg}} = \frac{1}{T}\int_0^T \frac{u^2(t)}{R_L}\mathrm{d}t, \tag{1}$$

where T represents the duration of the step. The mean power was averaged by the ten steps to find a unique (final) value. This procedure was repeated for the following loads: 10 kΩ, 100 kΩ, 560 kΩ, 820 kΩ, 1 MΩ, 1.2 MΩ, 1.5 MΩ, 1.8 MΩ, 2.2 MΩ, 3.3 MΩ, 4.7 MΩ, 8.2 MΩ, and 10 MΩ.

A maximum value of p_{avg} = 93.5 μW was obtained for a load R_L = 1.8 MΩ. This resistance is the matched load for one piezoelectric element, for which there is a maximum power transfer from the piezoelectric element to the load, according to the maximum power transfer theorem. This value of resistance is in line with previous studies.

2.4 Placement under the foot

The insole was divided into three regions as seen in Figure 5: region 1 between the metatarsals and phalanges, region 2 in the outer side, and region 3 in the heel. Each region was populated with several piezoelectric elements enriched with PLA structures: four elements in region 1, three elements in region 2, and seven elements in region 3. The elements in each zone were all connected in parallel ending on a 2-wire connector. Tests were carried out to find the best way to connect the three regions: connect them all in parallel, on a

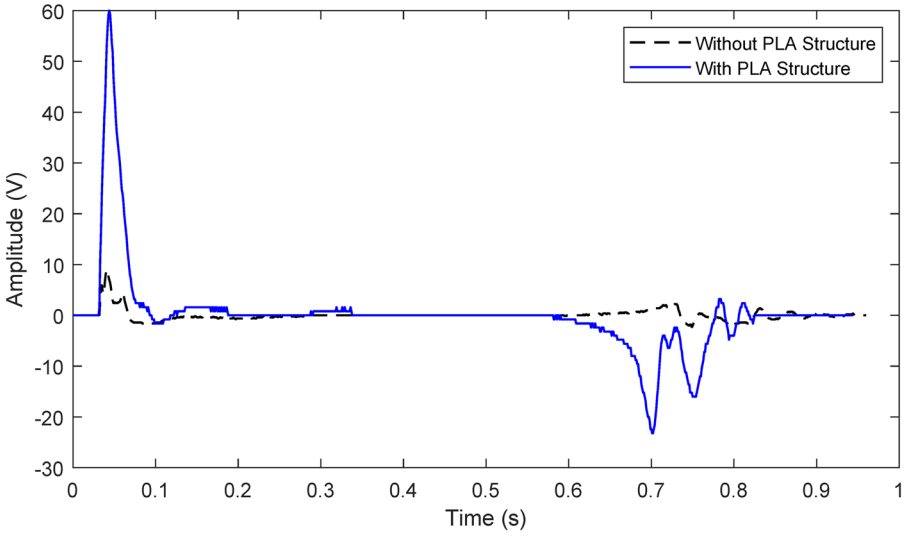

Figure 4: Voltage waveforms acquired during a single step without PLA structure (dashed line) and with the PLA structure (full line).

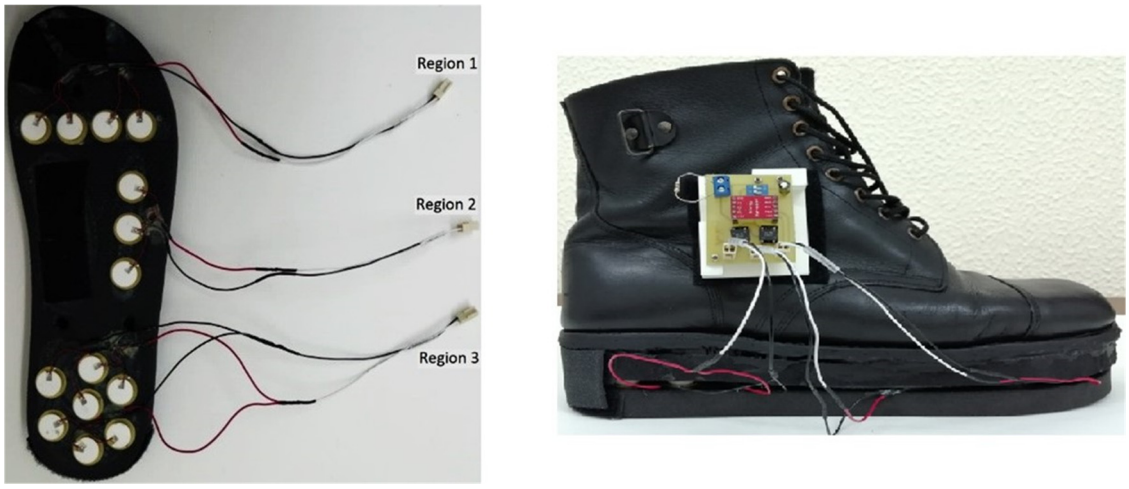

Figure 5: Distribution of piezoelectric elements over the insole.

single pair, and then collect the energy generated, or collect the energy of each zone separately.

The tests followed the same methodology of Section 2.3: the same typical user, the same series of ten "normal" steps, and the same digital scope acquiring waveforms. Since the scope had only two channels, we had to combine the regions in pairs: 1–2, 1–3, and 2–3. For each combination, we acquired waveforms when the regions were connected in parallel (Figure 6) or separately (Figure 7). As can be seen in Figure 7, there is a significant phase delay between the voltage waveforms generated in different regions of the foot: this result is in accordance with typical human gait dynamics, where different foot regions touch the ground at distinct instants (Perry & Burnfield 2010). As a consequence, due to this phase delay, there is some negative interference when piezoelectric elements from different regions are connected in parallel (e.g., in Figure 7, around t = 0.5 s, the positive voltage generated by region 1 cancels the negative voltage generated by region 3 if the piezoelectric elements from these two regions are connected in parallel – Figure 6). To prevent this undesired effect, we can provide a different conditioning circuit for each region, but this solution comes at a cost of additional power losses. To maximize the energy harvested in each step, we analyzed different connection topologies: the results are presented in the following section.

2.5 Conditioning circuit

The conditioning circuit is needed to collect the electricity generated by the piezoelectric elements, store it on a capacitor or battery, and then make it available in a regulated way.

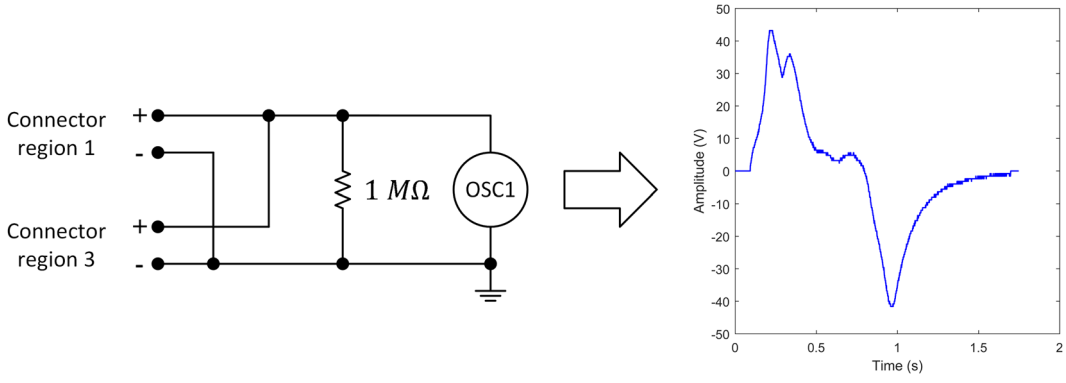

Figure 6: Combination of regions 1–3: regions connected in parallel. All voltages were acquired using a 10× attenuation probe. The same arrangement was made for combinations 1–2 and 2–3.

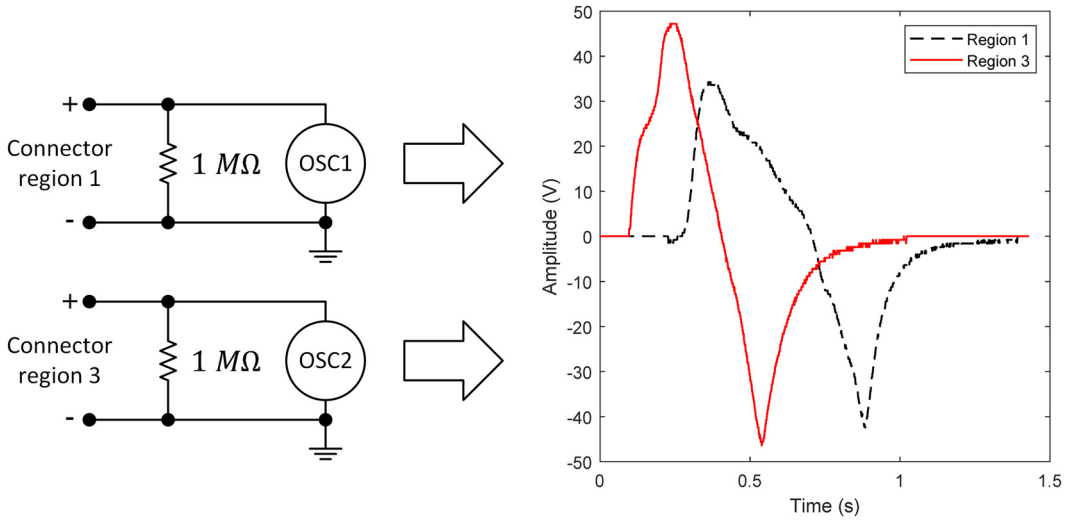

Figure 7: Combination of regions 1–3: regions connected separately, each one with its own load resistor and scope channel. All voltages were acquired using a 10× attenuation probe. The same arrangement was made for combinations 1–2 and 2–3.

In the present case, the conditioning circuit was built around the integrated circuit LTC3588-1 from Linear Technology, which integrates a low-loss full-wave bridge rectifier and a high-efficiency buck converter. This chip forms a complete energy-harvesting solution optimized for high-output impedance energy sources such as piezoelectric transducers. The circuit is able to provide four regulated, pin-selectable, output voltages (1.8, 2.5, 3.3, and 3.6 V) with up to 100 mA of continuous output current. External capacitors can be sized to store more incoming charge (input capacitor) and to service higher output current bursts (output capacitor).

The circuit, shown in Figure 8, includes two external full-wave bridge rectifiers and a breakout board from SparkFun (SparkFun 2023) that implements the typical application circuit of LTC3588-1. The external bridges rectify the electricity generated by the piezoelectric elements of regions 2 and 3, while an internal bridge (inside the LTC3588-1) rectifies the electricity generated by the

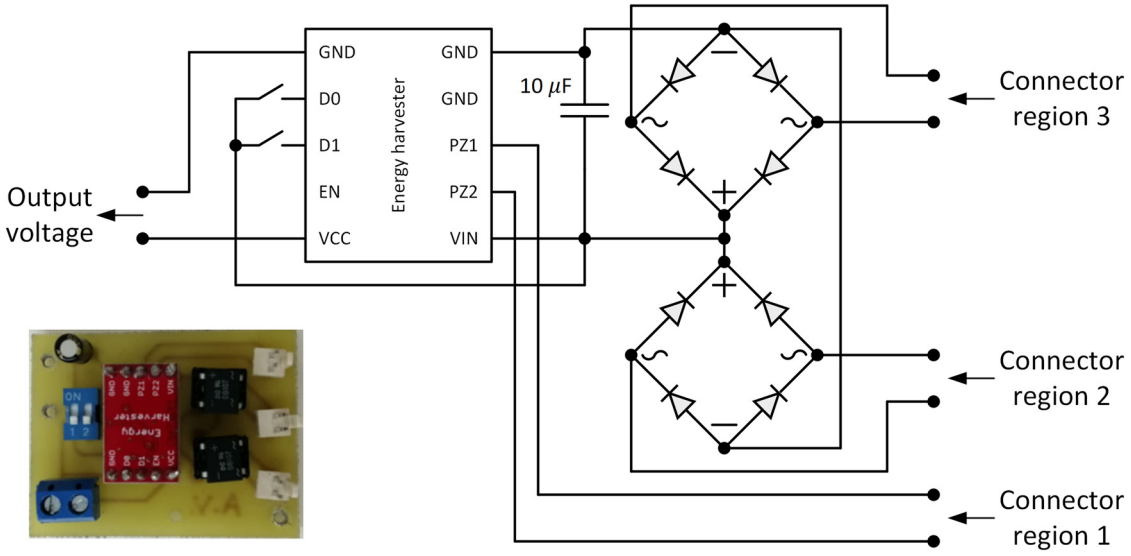

Figure 8: Piezoelectric generator printed-circuit board (PCB) and corresponding schematics.

Table 2: Energy generated per step: regions connected in parallel and regions connected separately

Combination	Mode	Energy (μJ)	p_{avg} (μW)
1–2	In parallel	475	374
	Separated	378	354
1–3	In parallel	516	313
	Separated	644	588
2–3	In parallel	548	369
	Separated	577	523
1–2–3	In parallel	703	401
	Separated	801	747

piezoelectric elements of region 1. The diodes prevent the current from flowing backward, thus making the regions work separately, isolated from each other. The input maximum voltage is limited to 20 V by a Zener diode (inside the LTC3588-1). The input capacitor was set to 10 μF and the output capacitor, not visible in the schema, was set to 4.7 μF. The output capacitor's main role is to flatten the output-regulated voltage, while the input capacitor acts as an energy reservoir. In general, a larger input capacitance value allows us to store more energy before reaching the 20 V voltage limit but, on the other hand, the circuit takes more time to charge and to provide a regulated voltage at its output in the warm-up phase. The input pins D0 and D1 select one of the four possible output voltages, and the output pin EN signals the presence of a regulated voltage at the output.

3 Results

To evaluate the best connection topology for the piezoelectric elements distributed across the three regions depicted in Figure 5, we performed a series of tests where we connected these elements to a 1 MΩ load resistor in different configurations:

- Two regions connected in parallel (regions 1–2, 1–3, and 2–3), according to Figure 6;
- Two regions connected separately (regions 1–2, 1–3, and 2–3), each one to a different load resistor, according to Figure 7;
- All three regions (regions 1–2–3) connected in parallel to the same load or separately to a different load resistor.

The mean power of each step was computed according to (1) and then averaged through the ten steps, leading to the results presented in Table 2 and the waveforms depicted in Figures 9–11.

Looking at the waveforms registered and the results obtained, we can make the following observations:

- The waveforms last longer when the regions are connected in parallel (the voltage signal in Figure 10 extends further in time than the voltage signal in Figure 9). This is justified by the fact that there are more capacities in parallel and that they take longer to charge and discharge;
- The voltages generated by regions 1 and 3 are out of phase, with the signal from region 3 (heel) in advance to the signal from region 1 (between the metatarsals and phalanges). The time lags observed in the combinations

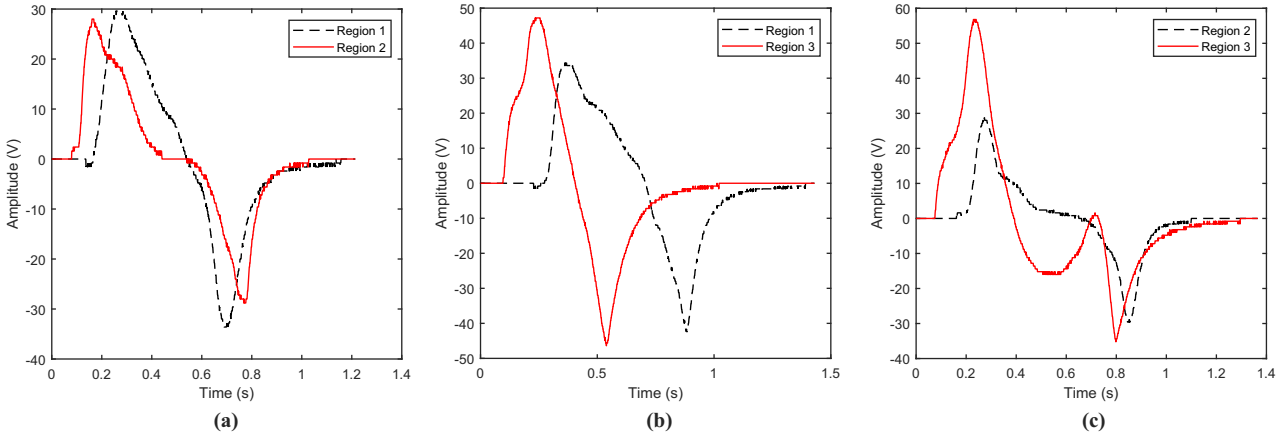

Figure 9: Examples of voltage waveforms generated by piezoelectric elements in a single step, each region connected separately to its 1 MΩ load resistor: (a) regions 1 and 2, (b) regions 1 and 3, and (c) regions 2 and 3.

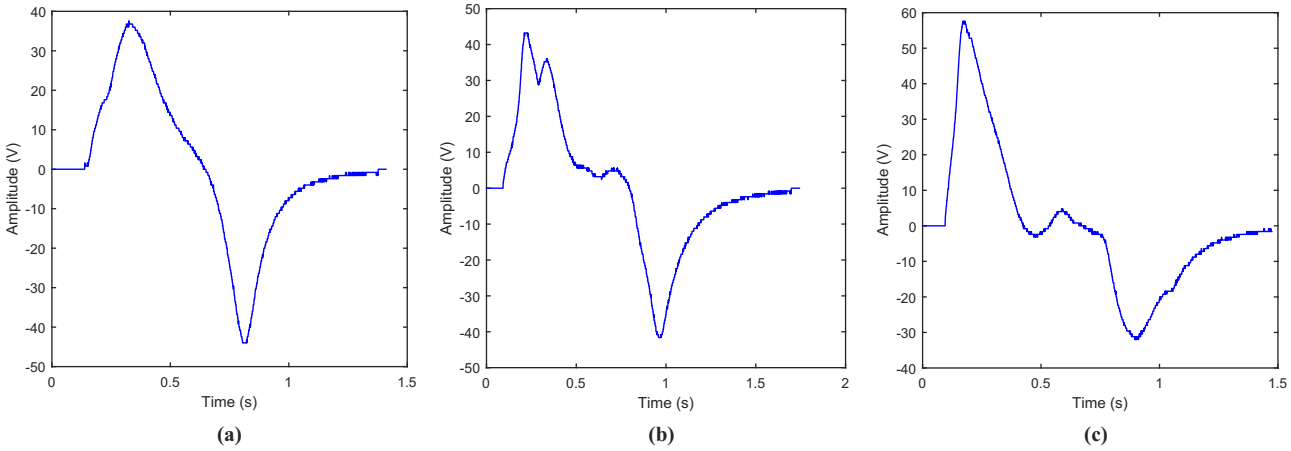

Figure 10: Examples of voltage waveforms generated by the piezoelectric elements in a single step, with regions connected in parallel to a single 1 MΩ load resistor: (a) regions 1 and 2, (b) regions 1 and 3, and (c) regions 2 and 3.

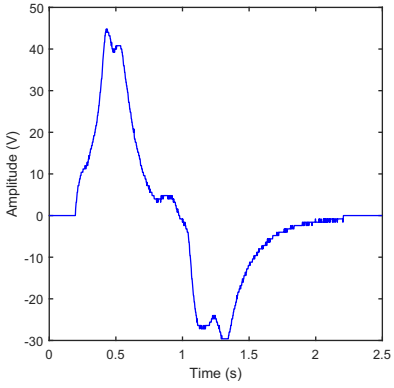

Figure 11: Example of a voltage waveform generated by piezoelectric elements in a single step, with all three regions connected in parallel to a single 1 MΩ load resistor.

1–2 and 2–3 are much smaller. This is in accordance with the gait phases described in the literature (Perry & Burnfield 2010), which state that heel is the first to touch the ground and the phalanges are the last to leave the ground;

- In general, separate, independent regions generate more power than regions connected in parallel. The exception is the combination 1–2 but just barely. Since the signals of the different regions are out of phase, it is possible that, in some moments, the energy generated in one region (e.g., region 3) is absorbed (dissipated) in the regions that are resting (e.g., region 1).

Based on these observations, we concluded that the energy harvested was maximized when the piezoelectric elements were connected separately, each one to its own

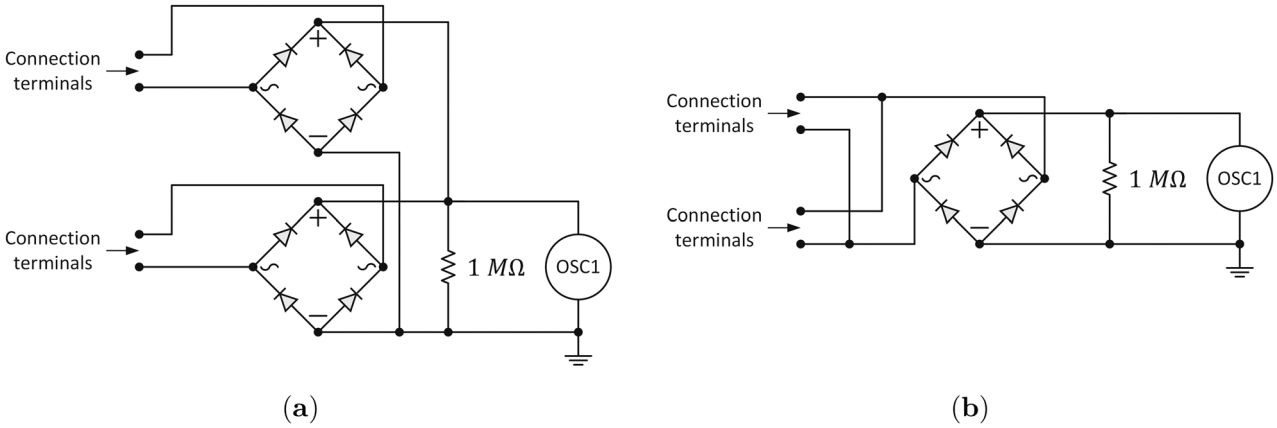

Figure 12: Circuit schematics for piezoelectric voltage rectification: (a) each region voltage is rectified before the parallel connection to the 1 MΩ load resistor and (b) the piezoelectric elements are connected in parallel before rectification.

load, in order to minimize the energy transfer between piezoelectric elements from one foot region to another.

In the next experiment, we studied the energy harvested when the voltage originating on each region was first rectified using a full-bridge rectifier. We also analyzed the parallel connection between regions before voltage rectification, for comparison purposes. The connection schematics are depicted in Figure 12 (we used the same 1 MΩ load resistor as in the previous experiment). Numerical results are presented in Table 3.

The energy generated by the typical user, per foot and per step, on average, considering the rectification of the voltage generated in the three regions before feeding a 1 MΩ load resistor, was equal to 875 μJ. This value is a good indicator of the energy potential of a single step, and it is line with previous studies aforementioned in Section 1: it is above the result obtained by Fan et al. (2017) (287 μJ) and below the result obtained by Zhao & You (2014) (1,000 μJ).

The full prototype was finally mounted and installed in the boot, ready to be stimulated by the typical user. The output of the energy harvester (pin VCC in Figure 8) was connected to a simple 1 MΩ resistor acting as a load. Pins D1 and D0 were connected to HIGH and LOW, respectively, to generate a regulated output voltage of 3.3 V. Pins VCC and VIN were connected to the digital scope using 10× attenuation probes to minimize the load effect. The user made a series of 100 steps (approximately 150 s) leading to the waveforms presented in Figure 13.

The VIN voltage is always positive because it is rectified by the full-wave bridges. Its value rises as the charge generated by the piezoelectric elements is stored in the input capacitor (10 μF).

Two steps were enough for the output voltage to be considered valid (pin EN equal to HIGH). While the user was making steps, the output voltage remained valid, regulated, equal to 3.3 V. After the user stopped walking, the input capacitor discharged gradually, to the point where the buck converter was unable to guarantee a regulated output voltage, after around 50 s. Larger capacitors would hold charge longer, and on a practical application, it would be probably advisable to increase the input capacitance to ensure that the output voltage was available, for some specified time and under a given nominal output load, while the soldier was at rest.

Table 3: Energy generated per step: voltage rectification before and after parallel connection between different regions

Combination	Mode	Energy (μJ)	p_{avg} (μW)
1–2	Single rectifier	462	312
	One rectifier per region	446	293
1–3	Single rectifier	501	281
	One rectifier per region	737	453
2–3	Single rectifier	515	329
	One rectifier per region	568	397
1–2–3	Single rectifier	661	376
	One rectifier per region	875	497

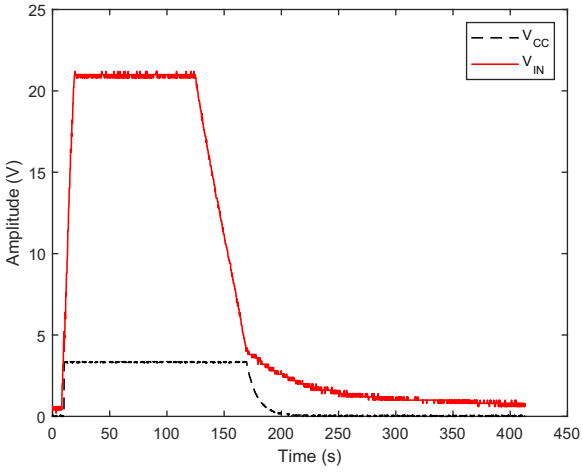

Figure 13: Input and output voltages of the energy harvester.

4 Discussion

This study described the development of a piezoelectric generator intended to harvest energy from the soldier's gait. The generator was optimized regarding the deformation of the piezoelectric elements, their placement under the foot, and their connection to the conditioning circuit. Experiments were conducted to find the matched load and to quantify the energy generated per step. The results are promising when compared to state-of-the-art works.

The energy harvested on each step, in average, is about 875 μJ. Walking 1 h, at a pace of 40 steps/min, leads to 2.1 J of energy, enough to supply a 3.3 V device consuming 10 mA for around a minute. To these values, we must subtract the losses associated with the operation of the energy harvester (LTC3588-1). Even so, this device is interesting for any situation that requires emergency power on the battlefield (e.g., to trigger a device, to call for rescue, to acquire localization).

The prototype worked fine, with all the waveforms looking as expected. The output voltage became valid very quickly and remained regulated at 3.3 V while the user was walking. The time between starting to march

and having a valid output and the time between stopping and no longer having a valid output depend on the values of the two capacitors. Finally, it should be underlined that the prototype is low cost, totally made of commercial off-the-shelf components. In our case, we spent around 30 € for the conditioning circuit (including the energy harvester, two rectifying bridges, passive components, PCB, etc.), and 7 € for the piezoelectric elements (14 × 0.5 €).

Further improvements include the miniaturization of the prototype, making possible a seamless integration into military boots, and the experimentation of more efficient piezoelectric materials. The harvesting of energy on other parts of the body, including legs and arms, is also a point of interest.

Funding information: Authors states no funding involved.

Author contributions: Conceptualization, J.V., B.D. and V.V.; methodology, B.D. and V.V.; hardware, J.V and V.V.; validation, B.D. and V.V.; formal analysis, B.D. and V.V.; investigation, J.V., B.D. and V.V.; resources, J.V. and V.V.; writing – original draft preparation, J.V.; writing – review and editing, B.D. and V.V.; supervision, B.D. and V.V.. All authors have read and agreed to the published version of the manuscript.

Conflict of interest: The authors states no conflict of interest.

Research ethics: Not applicable.

Data availability statement: The raw data can be obtained on request from the corresponding author.

References

Fan K., Liu Z., Liu H., Wang L., Zhu Y., and Yu B. (2017). Scavenging energy from human walking through a shoe-mounted piezoelectric harvester, *Appl. Phys. Lett.* vol. 110, no. 14, p. 143902.

Granstrom J., Feenstra J., Sodano H. A., and Farinholt K. (2007). Energy harvesting from a backpack instrumented with piezoelectric shoulder straps, *Smart Materials Struct.*, vol. 16, no. 5, p. 1810.

Harper J. (2015). The army wants to power up dismounted soldiers, *National Defense*, vol. 100, no. 743, pp. 42–45.

Heywang W., Lubitz K., and Wersing W. (2008). *Piezoelectricity: evolution and future of a technology*, Springer Science & Business Media, Berlin/Heidelberg, Germany.

Howells C. A. (2009). Piezoelectric energy harvesting, *Energy Conversion and Management*, vol. 50, no. 7, pp. 1847–1850.

Hwang S. J., Jung H. J., Kim J. H., Ahn J. H., Song D., Song Y., et al. (2015). Designing and manufacturing a piezoelectric tile for harvesting energy from footsteps, *Current Appl. Phys.*, vol. 15, no. 6, pp. 669–674.

Ishida K., Huang T.-C., Honda K., Shinozuka Y., Fuketa H., Yokota T., et al. (2013). Insole pedometer with piezoelectric energy harvester and 2 v organic circuits, *IEEE J. Solid-State Circuits*, vol. 48, no. 1, pp. 255–264.

Jung W.-S., Lee M.-J., Kang M.-G., Moon H. G., Yoon S.-J., Baek S.-H., and Kang C.-Y. (2015), Powerful curved piezoelectric generator for wearable applications, *Nano Energy*, vol. 13, pp. 174–181.

Kim H. W., Priya S., Uchino K., and Newnham R. E. (2005). Piezoelectric energy harvesting under high pre-stressed cyclic vibrations, *J. Electroceramics*, vol. 15, pp. 27–34.

Kuang Y., Yang Z., and Zhu M. (2016). Design and characterisation of a piezoelectric knee-joint energy harvester with frequency up-conversion through magnetic plucking, *Smart Materials Struct.*, vol. 25, no. 8, pp. 085029.

Perry J. and Burnfield J. M. (2010). *Gait analyzis. Normal and pathological function*, 2nd edition. SLACK Incorporated.

Pointon A. (1982). Piezoelectric devices, in: *IEE Proceedings A (Physical Science, Measurement and Instrumentation, Management and Education, Reviews)*, vol. 129, no. 5, pp. 285–307.

Raadschelders J. and Schmal D. (1999). *Energy sources for soldier modernisation programme systems (overzicht van ontwikkelingen op het gebied van raagbare energieopslag en energieopwekking)*, Technical report, TNO institute of Environmental Sciences, Energy Research and Process Innovation, The Netherlands, Available online: https://apps.dtic.mil/sti/pdfs/ADA372686.pdf. Accessed on January 8, 2024.

Rocha J. G., Goncalves L. M., Rocha P., Silva M. P., and Lanceros-Mendez S. (2009). Energy harvesting from piezoelectric materials fully integrated in footwear, *IEEE Trans. Industr. Electronics*. vol. 57, no. 3, pp. 813–819.

Sezer N. and Koç M. (2021). A comprehensive review on the state-of-the-art of piezoelectric energy harvesting, *Nano Energy*, vol. 80, p. 105567.

Shenck N. and Paradiso J. (2001). Energy scavenging with shoe-mounted piezoelectrics, *IEEE Micro*, vol. 21, no. 3, pp. 30–42.

SparkFun. Sparkfun energy harvester breakout - ltc3588. Available online: https://www.sparkfun.com/products/9946. Accessed on October 10, 2023.

Swanner J., Bito J., Nichols G., He X., Hewett J., and Tentzeris M. M. (2017). Integrating multiple energy harvesting systems for department of defense applications, In EESAT Conference-Evolution & Revolution.

Zhao J. and You Z. (2014). A shoe-embedded piezoelectric energy harvester for wearable sensors, *Sensors*, vol. 14, no. 7, pp. 12497–12510.